

APRIL 24 2023

Comparison of visual and passive acoustic estimates of beaked whale density off El Hierro, Canary Islands

P. Arranz; D. Miranda; K. C. Gkikopoulou; ... et. al



J Acoust Soc Am 153, 2469 (2023)

<https://doi.org/10.1121/10.0017921>



View
Online



Export
Citation

CrossMark

Related Content

Acoustic detection of beaked whales from autonomous recording buoys

J Acoust Soc Am (May 2008)

Spatio-temporal variation in click production rates of beaked whales: Implications for passive acoustic density estimation

J Acoust Soc Am (March 2017)

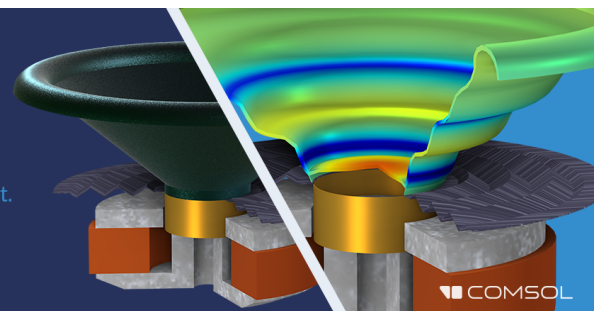
Echolocation click parameters of short-finned pilot whales (*Globicephala macrorhynchus*) in the wild

J Acoust Soc Am (March 2021)

Take the Lead in Acoustics


The ability to account for coupled physics phenomena lets you predict, optimize, and virtually test a design under real-world conditions – even before a first prototype is built.

» Learn more about COMSOL Multiphysics®



COMSOL

Comparison of visual and passive acoustic estimates of beaked whale density off El Hierro, Canary Islands

P. Arranz,^{1,a),b)}  D. Miranda,¹ K. C. Gkikopoulou,² A. Cardona,² J. Alcazar,¹ N. Aguilar de Soto,¹ L. Thomas,³ and T. A. Marques^{4,b)}

¹BIOECOMAC, Departamento de Biología Animal, Edafología y Geología. Universidad de La Laguna. Avenida Astrofísico F. Sánchez, s/n. 38206 San Cristóbal de La Laguna, Tenerife, Spain

²Sea Mammal Research Unit, Scottish Oceans Institute, University of St Andrews, KY16 8LB St Andrews, Scotland

³Centre for Research into Ecological and Environmental Modelling, University of St Andrews, KY16 8LB St Andrews, Scotland

⁴Departamento de Biología Animal, Centro de Estatística e Aplicações, Faculdade de Ciências, Universidade de Lisboa, 1749-016, Campo Grande, Lisboa, Portugal

ABSTRACT:

Passive acoustic monitoring (PAM) offers considerable potential for density estimation of cryptic cetaceans, such as beaked whales. However, comparative studies on the accuracy of PAM density estimates from these species are lacking. Concurrent, low-cost drifting PAM, with SoundTraps suspended at 200 m depth, and land-based sightings, were conducted off the Canary Islands. Beaked whale density was estimated using a cue-count method, with click production rate and the probability of click detection derived from digital acoustic recording tags (DTags), and distance sampling techniques, adapted to fixed-point visual surveys. Of 32 870 detections obtained throughout 206 h of PAM recordings, 68% were classified as “certain” beaked whale clicks. Acoustic detection probability was 0.15 [coefficient variation (CV) 0.24] and click production rate was 0.46 clicks s⁻¹ (CV 0.05). PAM density estimates were in the range of 21.5 or 48.6 whales per 1000 km² [CV 0.50 or 0.44, 95% confidence interval (CI) 20.7–22.4 or 47–50.9], depending on whether “uncertain” clicks were considered. Density estimates from concurrent sightings resulted in 33.7 whales per 1000 km² (CV 0.77, 95% CI 8.9–50.5). Cue-count PAM methods under application provide reliable estimates of beaked whale density, over relatively long time periods and in realistic scenarios, as these match the concurrent density estimates obtained from visual observations. © 2023 Acoustical Society of America.

<https://doi.org/10.1121/10.0017921>

(Received 16 September 2022; revised 28 March 2023; accepted 6 April 2023; published online 24 April 2023)

[Editor: Aaron M. Thode]

Pages: 2469–2481

I. INTRODUCTION

Accurate and precise estimates of animal density are critical to inform wildlife management and conservation, and for effective real-time mitigation of anthropogenic disturbance on wild populations. Traditional methods to obtain such estimates typically involved visual methods based on detecting or capturing the animals (e.g., Buckland *et al.*, 2015; Williams *et al.*, 2002; Borchers and Efford, 2008). Visual survey methods are labor-intensive and can be challenging when animals occur at low density (Marques *et al.*, 2013).

An alternative is an indirect method, cue counting, where “cues” produced by the animals, like nests, dung, or sounds, are counted and converted into density estimates (Buckland and Handel, 2006; Marques *et al.*, 2009). Marques *et al.* (2013) provided an extensive overview of available cue-based methodological approaches. Passive acoustic monitoring (PAM) constitutes a cost-effective indirect method when sampling acoustically active taxa, particularly in habitats where human access is limited or that have poor visibility

conditions (Marques *et al.*, 2009; Deichmann *et al.*, 2017; Aodha *et al.*, 2018). Additionally, autonomous PAM recording platforms can be left in the field for extended periods, allowing studies to be conducted at larger temporal and spatial scales (Hagens *et al.*, 2018) than if dependent on human observers. Furthermore, acoustic cue detection and classification from PAM data can be calibrated and automated, reducing time needed for data collection and processing. When estimating animal density using cue counting, multipliers are needed to convert counts of detected cues to animal density, including cue production rate, proportion of false positive–negative detections, and probability of cue detection or effective sampling area. However, we are aware of only one case where PAM-based density estimation has been validated by comparison with a simultaneous reliable non-acoustic method; Phillips (2016) used a small, shallow bay in Florida to compare several PAM density estimates for the common bottlenose dolphin (*Tursiops truncatus*) with complete counts made by visual observers.

Beaked whales are a widespread family of inconspicuous and relatively unknown odontocetes, particularly sensitive to anthropogenic disturbance (Cox *et al.*, 2006). They perform long deep dives, with maximum dive depths and

^{a)}Electronic email: arranz@ull.edu.es

^{b)}Also at: Centre for Research into Ecological and Environmental Modelling, University of St Andrews, KY16 8LB St Andrews, Scotland.

durations of 1890 m and 85 min for Cuvier’s beaked whale (*Ziphius cavirostris*) and 1250 m and 57 min for Blainville’s beaked whales (*Mesoplodon densirostris*) (Tyack *et al.*, 2006), during which they are vocally active around 20% of the time (Arranz *et al.*, 2011). They emit characteristic frequency-modulated echolocation clicks, which facilitates detection and species identification from acoustic recordings (Johnson *et al.*, 2006; Zimmer *et al.*, 2005). Beaked whale density estimation based on visual methods has proven difficult due to their typical oceanic distribution and low detection rates during visual line-transect surveys (Barlow *et al.*, 2013). Several studies have derived density estimates using acoustic detections of beaked whales (Marques *et al.*, 2009; Moretti *et al.*, 2006; Ward *et al.*, 2011; Hildebrand *et al.*, 2015; Barlow *et al.*, 2022).

Resident populations of Blainvillés (*Mesoplodon densirostris*) and Cuvier’s (*Ziphius cavirostris*) beaked whales can be found year-round off El Hierro, Canary Islands, Spain (Reyes, 2018). A deep-water bay on the leeward side of the island can be simultaneously monitored with PAM recorders and by observers located on land-based platforms on the sea cliffs (Arranz *et al.*, 2013). This provides a

unique opportunity to estimate visually the number of animals present in the bay and hence compare visual- and acoustic-based density estimates from concurrent PAM recordings. Here, we quantify acoustic parameters required for beaked whale density estimation using PAM data and use these to provide acoustic density estimates that are contrasted against concurrent visual land-based survey data.

II. METHODS

A. Field data collection

Four drifting passive acoustic sensors (SoundTrap ST 300, Ocean Instruments, New Zealand) were deployed daily for 45 survey days between August 28, 2016 and May 8, 2017 on the leeward side of El Hierro, following a depth-stratified sampling design, with two in shallower and two in deeper waters [Fig. 1(a)]. The survey area is a deep-water bay facing southwest, protected from prevalent wind and ocean currents. SoundTraps were initially located ~3 km apart and suspended at 200 m depth from a weighted rope connected to a surface buoy equipped with a 3 G

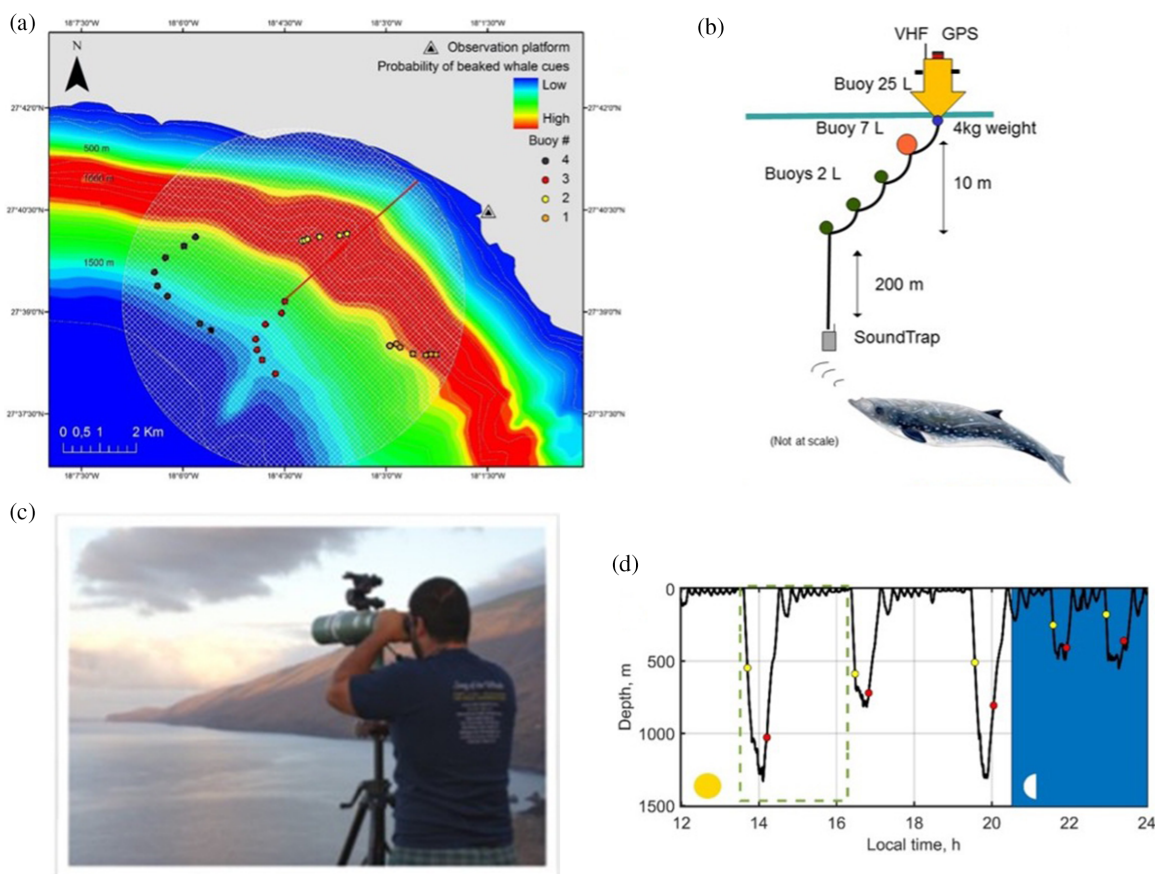


FIG. 1. (Color online) Combined PAM and land-based visual field experiments off El Hierro island, Canary Islands. (a) Hourly location of SoundTraps #1–4 on October 18, 2016 from 8:30 AM to 3 PM local time. White hatched area shows area used to determine detection probability for the single SoundTrap at the center of this area; red line shows maximum detection radius. Colored background shows assumed animal density, used in calculating acoustic detection probability (see Methods); white lines show bathymetry contours. (b) Drifting sensors used in this study. (c) Observer on the land survey platform overlooking the deep-water bay. (d) Dive profile (a single dive cycle is framed in the green dashed box) of a Blainvillés beaked whale recorded using DTag in El Hierro showing periods of start (yellow dots) and end (red dots) of clicking. Daytime is indicated by a sun icon and nighttime by a half-moon and blue background. Whale drawn by Chloe Yzard.

global positioning satellite (GPS) (Tractive, Austria) and a very-high frequency (VHF) transmitter antenna (ATS, Minneapolis, MN) for tracking and recovery [Fig. 1(b)]. SoundTraps recorded at a sampling rate of 288 kHz [16 bit, flat (± 2 dB) frequency response from 0.02–100 kHz, clip level 175 dB re 1 μ Pa, high gain], and the GPS location of each of these was recorded every hour.

Concurrently, visual surveys overlooking the same area were conducted from coastal cliffs using two identical platforms (119 m above sea level, 100 m apart, 27.67482° N, -18.02535° W, and 27.6732° N, -18.02400° W), with a field of view spanning true bearings between 160° and 294° [Fig. 1(c)]. Visual effort typically started at 8:30 AM local time (WEST), once the four SoundTraps were placed and had started recording, and ended at 3 PM local time, once the first SoundTrap was recovered. Mean combined survey effort was 6.2 h/day [standard deviation (SD) 1.9 h/day]. This diurnal sampling pattern was selected to avoid the sun glare from the late afternoon (when solar incidence angle decreased) which drastically reduces visibility from the observation platforms. At each observation platform, two observers used 7 × 50 binoculars, which included both compass and ocular reticules, to cover visually half of the compass area each with a 10° overlap (hereafter referred to as a “scan”). Simultaneously, a central observer covered the full visible horizon with 15 × 80 Fujinon binoculars, also equipped with compass and ocular reticules, tripod-mounted to enable more accurate reticle distance estimation (Arranz *et al.*, 2013). Each observer dedicated 2 min on average per scan and shifted position with the next observer position every 30 min, with a “resting/data logger” position every 1.5 h. The data logger recorded the following environmental data at the start of their 30 min shift: sea state within the study area (0–4 on the Douglas scale), swell (<0.5, 0.5–1, >1 m), weather conditions (sunny, cloudy, light rain, rain, foggy, haze, night), visibility (1–3 from low to high) and boat presence, number, and type (fishing, diving, yachts, and ferries). In addition, visual sightings data (start and end time, bearing, reticule, number of animals in the group, social composition, and behavior) were recorded for each beaked whale detection. Bearing and reticule of recorded groups were used to georeference the sightings (Lerczak and Hobbs, 1998).

A subset of sampling days was considered for further analysis, based on the following criteria: sea state <2, high visibility, drift of the acoustic sensors <1 nm. This resulted in 8 from 45 total survey days (~ 20%) being selected for the analysis.

B. Field data analyses

Acoustic data were analyzed using Matlab R2017a (Mathworks, US) and PAMGUARD (Gillespie *et al.*, 2009) with a specific configuration that simultaneously ran two beaked whale click energy band ratio classifiers. The first classifier was set using the PAMGUARD default for beaked whales, which is based on the number of times the waveform crosses zero in the x axis (i.e., the sign of the mathematical function changes from positive to negative or vice versa), the signal’s peak, and mean frequencies. The second was a custom classifier, built based on the waveform’s number of times crossing zero and the signal’s peak frequency and length (Table I). To minimize false-positive detections, four PAM operators visually checked the full detectors’ outputs, manually assigning the category of “certain” or “uncertain” to each beaked whale click automatically detected by the classifier, based on the inspection of each click’s waveform, spectrum, and Wigner plot (Johnson *et al.*, 2006). Clicks that did not qualify were considered “non-beaked whale” clicks and were therefore discarded from the final analysis.

Visual sighting data were divided into 2 min “snapshots.” This time window is consistent with the average surfacing time of beaked whales (Arranz *et al.*, 2011), reducing the possibility of double-counting the same group within a snapshot. The number of snapshots was therefore considered the measure of effort when estimating density from visual surveys.

A “visual sighting” from land-based surveys was defined as the observation of a beaked whale group at the surface (i.e., one or more beaked whales swimming in close spatial and temporal association). A rule-based “duplicate” categorization (Schweder and Hjort, 1996) was applied to suspected duplicate sightings across the two visual platforms. If the start time of suspected duplicate sightings matched (± 2 min), these were considered as “certain” duplicates if the bearing ($\pm 5^\circ$), reticules (± 2), and individuals (± 2) also matched, considered as “probable” if only two of these three criteria matched, and considered as “non-duplicates” if only one criterion matched. Sightings were not analyzed at a species level to avoid potential errors in species identification at long distances and variable ambient conditions.

C. PAM density estimation

Considering passive acoustic data from the Soundtraps, density of beaked whales, pooled-across species, was estimated using a cue-counting method, which uses detected

TABLE I. Configuration parameters for each of the energy-ratio classifiers used for classifying beaked whale clicks from passive acoustic recordings. This table shows the settings used in PAMGUARD for default and custom click classifiers (Caillat, 2018).

Classifier type	Control band (kHz)	Test band (kHz)	No. of zero crossings	Click length (ms)	Peak frequency (kHz)	Mean frequency (kHz)
Energy ratio default	12–24	24–48	7–50	—	25–48	25–48
Energy ratio custom	12–24/45–60	24–45	6–100	0.04–70	25–45	—

individual clicks as the cue of interest (Marques *et al.*, 2009; Marques *et al.*, 2013). Density estimates (\hat{D}) were obtained for each sensor and hour as follows, and the results averaged per sensor across recording periods to estimate an overall density across sensors:

$$\hat{D} = \frac{n}{K \pi w^2 \hat{r} T \hat{P}}, \quad (1)$$

where n is the number of detected clicks, K is the number of sensors, w is the maximum detection distance at which it is believed to be possible to detect a click, \hat{r} is the estimated click production rate, T is the survey time, and \hat{P} is the estimated average detection probability of a click within distance w of a sensor per sensor and hour [see Eq. (2)]. Below, we describe how we estimated each of the random components in Eq. (1). The variance of the average density was estimated from the empirical variance of $N = 1000$ bootstrap resamples of acoustic multipliers, and confidence intervals were calculated via the percentile method.

1. Click production rate

The rate at which beaked whales produce clicks was estimated from independent data from animal-borne motion acoustic sensors and digital acoustic recording tags (DTags) (Johnson and Tyack, 2003). Blainville’s beaked whale data were collected in the same study area, from 2003 to 2010 [Fig. 1(d)] (Gkikopoulou, 2018) (See supplementary material for raw data used to estimate Blainville’s and Cuvier’s beaked whale click production, dive cycle length, and the resulting click rate from DTag recordings in Table S1).¹ For Cuvier’s beaked whales, click rates used were from DTag data collected in the Liguria Sea (Italy) and the California basin (United States) from 2003 to 2013 (See supplementary material for raw data used to estimate Blainville’s and Cuvier’s beaked whale click production, dive cycle length, and the resulting click rate from DTag recordings in Table S1).¹ A supervised click detector (bandpass energy detector with a user-selected threshold) was used to identify individual clicks. Clicks from the tagged whale were distinguished from those of conspecifics based on consistency patterns of angle of arrival and click level (Arranz *et al.*, 2011). A joint mean “click production rate” was estimated for both species by averaging their corresponding cue rates weighted by the presence ratio of each species in the study area. This ratio was estimated as the proportion of individuals, both transient and resident, captured using photo identification (ID) techniques for each species over a 10-year period (48% and 52% of captures corresponding to Cuvier’s and Blainville’s beaked whales, respectively; see Reyes, 2018). The variance of this average cue rate was estimated from the empirical variance of bootstrap resamples, and confidence intervals were calculated via the percentile method. The sampling units used were the deep dives within each tag, sampled with probability equal to the proportion of each species in the study area estimated from the photo ID data. For this, we assume that baseline behavior of Cuvier’s beaked whale

from different geographical areas is comparable, based on the similar acoustic and dive behaviors that have been observed from whales tagged in Liguria and in Azores (Aguilar de Soto *et al.*, 2020).

2. Acoustic detection function

The average acoustic detection probability P is defined as the probability of detecting a beaked whale click given that the click is emitted within a horizontal circle of radius w from a given sensor. This was obtained by first estimating a detection function, which is a function relating the probability of click detection to horizontal distance between animal and sensor, and then averaging the detection function over the distribution of horizontal distances for each sensor. We describe how the detection function was obtained in this section, and how the averaging was done in Sec. II C 3.

The detection function was estimated from a regression analysis on independent data gathered in El Hierro in spring and autumn 2018 and 2019, where a sample of nine Blainville’s beaked whales were fitted with DTags and simultaneously recorded on a PAM sensor (SoundTrap) placed at 200 m depth. Full details are given in Gkikopoulou (2018) and summarized here.

Clicks arriving from the tagged whale on the PAM recorder were identified using synchronized envelope plots. The direct distance (slant distance) of the whale to the hydrophone was estimated by computing the acoustic time of flight (Cato, 1998), after correcting for the clock offset, between DTag and acoustic receiver, using surface bounces of a subset of clicks. A Kalman filter was used to smooth the distance estimates and to predict distances at times when the animals’ produced clicks that were not detected in the envelope plot. The distances of each click were then translated into horizontal distances using the depth measurement from the DTag and the known depth of the PAM recorder. A beaked whale classifier, comprising a correlation detector using a signal template of a combination of on- and off-axis clicks, was run on the PAM data and was used for estimating the acoustic detection function (Gkikopoulou, 2018). The acoustic detection function was estimated using a generalized estimating equation (GEE) modelling framework in R (R Core Team, 2022). The response was a binary variable: whether each click was detected (1) or not detected (0) by the classifier. This was assumed to follow a Bernoulli distribution and was linked to explanatory variables via a logit link function. The explanatory variable was the horizontal distance between whale and PAM sensor. The fitted detection function was used to predict detection probability as a function of horizontal distance.

3. Acoustic detection probability

To obtain the average acoustic detection probability for each sensor in each hour, we averaged the detection function over the distribution of beaked whale locations within distance w of the sensor location. Beaked whales are not distributed uniformly in horizontal space at El Hierro, and we

TABLE II. Comparison of land- versus boat-based visual estimates of beaked whale group size. A total of 195 sightings of Blainvillés and Cuvier’s beaked whales recorded off El Hierro between 2003 and 2011 for which paired data were available.

	Boat-based counting	Land-based counting
Total beaked whale count	611	639
Beaked whale group size (mean, SD)	2.70, 1.77	2.84, 1.77

made use of the density surface estimated from earlier visual data by Arranz *et al.* (2013). Note that this dataset is independent of the visual dataset used to generate visual abundance estimates in the current study.

A grid of cells with 100 × 100 m resolution was created using the ArcMap 9.2 software (ESRI, Redlands, CA). The horizontal distance of the SoundTrap to each cell’s center position (m , obtained from the SoundTraps’ GPS location recorded every hour), was estimated. Detection probabilities, weighted by the density of beaked whales in the area, were obtained for each acoustic sensor and hourly location. The weighted detection probability (\hat{P}_w) was estimated as follows:

$$\hat{P}_w = \frac{\sum_{i:r(i) \leq m} \hat{d}(i)\hat{p}(r(i))}{\sum_{i:r(i) \leq m} \hat{d}(i)}, \tag{2}$$

where m is the horizontal distance of the SoundTrap to each cell’s center position, \hat{d} is the whale’s density estimated for the i th cell, \hat{p} is the acoustic detection function, $r(i)$ is the horizontal distance of the i th cell location to the sensor, and $i : r(i) \leq m$ denotes the set of cell locations such that the distance is less than or equal to m .

D. Visual density estimation

Density of beaked whales (\hat{D}) was also estimated from land-based visual observations using a Horvitz–Thompson type estimator (Horvitz and Thompson, 1952), as follows:

$$\hat{D} = \frac{\hat{s}z}{ak\hat{v}\hat{P}}, \tag{3}$$

where \hat{s} is an estimate of the mean group size, z is the number of groups seen per platform, a is the area monitored, k is the number of visual snapshot periods, \hat{v} is the probability of a group being at the surface at least once in a 2 min period (visual availability), and \hat{P} is the probability of visually detecting a beaked whale group at the surface (visual detection probability).

Below, we describe how we estimated each of the random components in Eq. (3).

1. Mean group size

Concurrent land- and boat-based beaked whale observations of whale groups, taken during the tagging experiments described in Sec. C 1, were used to correct average group size estimates recorded from land-based observations (\hat{s}). We assume for these the number of animals within the group were counted reliably from the tagging boat, and simultaneously estimated by observers located on land. The average group size ratio between land- and boat-based observations with group sizes ranging 1–11 individuals was used as a correction factor (Table II) [Fig. 2(a)].

2. Visual availability

The proportion of time that beaked whales spend at the sea surface and were therefore “available” to be visually detected by the observers (\hat{v}), was estimated using independent DTag datasets of both species (See the supplementary material for Table S1).¹ Consistent with the effort units and beaked whale surfacing periods, we computed the proportion of 2 min time windows during which the animal was “available” for visual detection, defined by the animal being at the surface (<1 m depth) for >4 s (this time threshold corresponds to the estimated average time a beaked whale spends at the surface during a surfacing–breathing event). We averaged values from both species to provide a

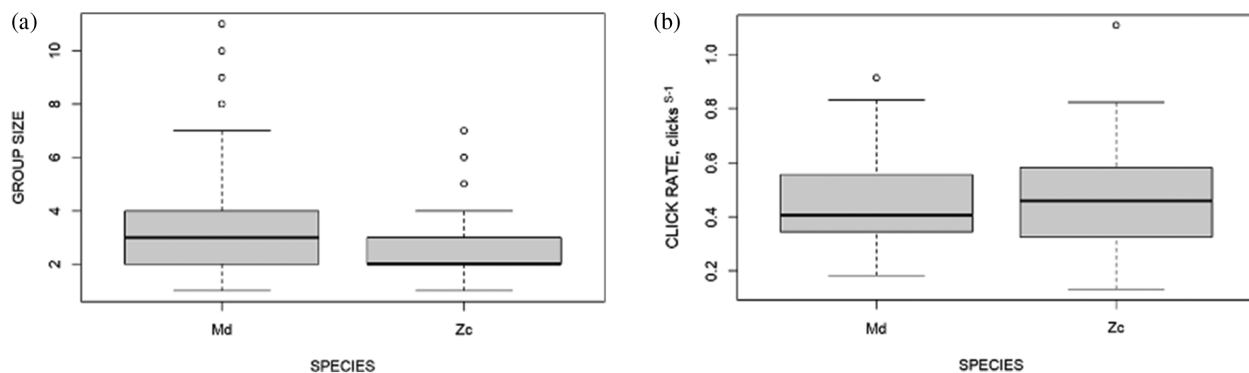


FIG. 2. Estimated group size (a) and click production rate (b) for Blainvillés (Md) and Cuvier’s beaked whale (Zc) species. Click rate was estimated using a bootstrap method with the deep dive cycle as re-sampling unit (N = 12 tagged Blainville’s beaked whales off El Hierro, N = 15 tagged Cuvier’s beaked whales tagged off California and Ligura). Average group size was estimated from boat-based beaked whale sightings off El Hierro during independent tagging experiments (N = 2291 sightings).

combined \hat{v} for Cuvier's and Blainvillés beaked whales sightings, weighted for the ratio of the species in the study area.

3. Visual detection probability

We considered two different approaches to estimate beaked whale group detection probability from the land-based data. The optimal approach depends on the assumptions one might be willing to make about the underlying observation and state processes. Model parameters were estimated using R v4.0.0 (R Core Team, 2022). The best model within each approach was selected based on Akaike information criteria (AIC) (Akaike, 1973). Model goodness-of-fit was evaluated using the X^2 statistic. In all cases, detection function estimates [hereafter $p(x)$] were computed using the full data set ($N = 45$ days), whereas density estimates were computed individually for each selected day ($N = 8$ days). The two approaches are described below.

a. Mark-recapture analysis We first conducted a mark-recapture (MR) analysis to fit a detection function for a double-observer point-transect survey, using distance from the whale to the observers as a covariate (Borchers *et al.*, 1998). Unlike conventional distance sampling, MR analysis does not assume a homogeneous density distribution of animals. However, it does assume that there is no un-modelled heterogeneity in the detection function. Ultimately, due to the poor fit of the detection function to the distribution of the data, this approach was not further developed.

b. Distance sampling with non-uniform whale distribution Since beaked whales in El Hierro are known to approach the sea-floor when feeding (Arranz *et al.*, 2011) and seabed depth is considered a key factor conditioning their distribution (Arranz *et al.*, 2013), a more robust approach was undertaken here. This consisted of applying a distance sampling analysis adapted to point-transects, in the presence of non-uniform animal distribution (unequal number of animals available for detection at all distances, expressed as the probability density function), that varies with some observable environmental feature (Cox *et al.*, 2013). This probability density function conveys information on the expected density of animal cues (i.e., surfacings) as a function of habitat variables across the survey area. To model the spatial relationship between beaked whale cue density and depth, a grid of cells (100×100 m resolution) spanning the survey area was created using ArcMap. Given the study area's steep bathymetry and the relatively large distances covered by each binocular reticule, this depth resolution was considered sufficient. Bearings and Euclidean distances to the observed beaked whale groups from land-based platforms were determined for each group and used to extract sighting locations. The projected grid cells were georeferenced in a Cartesian coordinate system (x, y), with x being the distance from the survey point parallel to the coast and y being perpendicular to x in the offshore direction (see

Arranz *et al.*, 2013 for details). For every cell, we extracted the seabed depth from a digital bathymetric map of the Canary Islands, with a vertical resolution of 50 m (IEO-IHM, 2001). The depth at each sighting location was the explanatory variable for the beaked whale cue density model, and the radial distance between the sighting and the observation platform was the explanatory variable for the detection probability model. Assuming that whales were distributed uniformly with respect to distance to the coast, we then adapted methods from Marques *et al.* (2010) and Cox *et al.* (2013) for estimating animal density when there is non-uniform cue density along the y axis direction and uniform along the x axis using Eq. S1 (See the supplementary material for a description of the general method and equations used to estimate a probability density function and visual detection probability for beaked whale groups from land-based observations).¹ The visual detection probability (i.e., probability of detection given one or more beaked whales at the surface available to be seen) was modeled as a function of radial distance alone using Eq. S2 (See the supplementary material for Eq. S2).

E. Variance estimation

1. Visual data

The variance of the visual density estimates was estimated via the delta method (Seber, 1982) using the following equation:

$$\text{var}(\hat{D}) = \hat{D}^2 \left(CV^2(\hat{P}_w) + CV^2(\hat{v}) + CV^2(\hat{s}) + CV^2(z) \right), \quad (4)$$

where \hat{D} is the estimated density, \hat{P}_w is the estimated visual detection probability, \hat{v} is the estimated availability bias, \hat{s} is the estimated mean group size, and z is the number of beaked whale groups per platform. $CV^2(x)$ denotes the squared coefficient of variation of x . Coefficient variation (CV) of visual detection probability was estimated using a non-parametric bootstrap (Arranz *et al.*, 2013) with 1000 resamples, using the day as a sampling unit. Availability bias CV was estimated from the standard error and the mean availability at the surface obtained for each tag record and species. Mean group size CV was estimated from the standard error and the mean of the beaked whale group size recorded per sighting for each survey day. CV of the number of beaked whale groups seen per platform was computed from the ratio of the standard error by the mean of the number of groups per 2 min scan recorded for each survey day.

2. Acoustic data

The sample variance of the acoustic density estimates was also computed using the delta method, with random components being the acoustic detection probability (\hat{P}_w), beaked whale dive cycle click rate (\hat{r}) and the number of beaked whale click detections (n):

TABLE III. Parameters used for the acoustic and visual beaked whale density estimation. Expressed as the mean, coefficient variation (CV) and 95% confidence intervals (95% CI). N , the number of detected clicks (all /certain); K , the number of sensors; w , the maximum detection distance (km); c , the click production rate (click sec^{-1}); T , the survey time (h); \hat{P}_w , the average weighted acoustic detection probability*; \hat{s} , the average group size (n whales); z , the number of groups seen per platform per day (averaged for platform 1 and 2); a , the area monitored (km^2); k the number of scans per platform (n scans); \hat{v} , the availability; \hat{P} , the visual detection probability. For presentation purposes, we report here \hat{P}_w , pooled-across sensors and time periods. However, density was estimated using \hat{P}_w for each sensor and hour location.

Data source	Parameter	Mean	CV	95% CI
Acoustic	n	1060/465	1.06/1.81	729–1391/278–652
	K	1	0	0
	w	2	0	0
	c	0.46	0.05	0.42–0.50
	T	6.67	0.14	6.32–7.03
	\hat{P}_w	0.15	0.24	0.15–0.16
Visual	\hat{s}	2.15	0.09	1.68–2.61
	z	30.87	1.05	10.91–50.83
	a	178	0	0
	k	216.87	0.11	196.07–237.67
	\hat{v}	0.25	0.05	0.023–0.29
	\hat{P}	0.20	0.15	0.08–0.49

$$\text{var}(\hat{D}) = \hat{D}^2 \left(CV^2(\hat{P}_w) + CV^2(\hat{r}) + CV^2(n) \right). \quad (5)$$

The CV of the acoustic detection probability was obtained from standard error and mean of the detection probability estimated per buoy for each survey day. The CV of beaked whale click detections was obtained from standard error and mean of the number of clicks detected per buoy for each survey day. The CV of the click production rate was estimated dividing the standard error by the mean of the click rates computed per dive and for each species using the bootstrap method (see Sec. C.1) (Table S1).¹

III. RESULTS

A. PAM density estimates

The estimated click rate (c) was 0.46 clicks s^{-1} (CV 0.05, 95% confidence interval (CI) 0.42–0.50); this is a

pooled-across-species weighted average of the individual cue rates for Cuvier’s and Blainville’s beaked whales, of 0.47 clicks s^{-1} (CV 0.05), and 0.46 clicks s^{-1} (CV 0.03), respectively [Fig. 2(b)] (Table III). The acoustic detection function computed for acoustic recorders is shown in Fig. 3. The average estimated probability of detecting a beaked whale click, pooled-across-sensors and hours (\hat{P}_w) was 0.15 (CV 0.24) (Table III). A total of 32 870 beaked whale click detections were recorded throughout the eight survey days selected for analysis, resulting in 53.2 h of sampled acoustic data from each SoundTrap (Fig. 4). The proportion of false-positive detections was 0.53 (CV 0.69), varying greatly in a non-discernible pattern across buoys within each day, depending mainly on concurrent dolphin (mostly *Tursiops truncatus*) presence in the study area. “Certain” click detection rates ranged from 37 to 199 clicks h^{-1} and were roughly comparable across sensors, although the proportion of “certain” click detections ranged widely throughout days (0.46–0.77) (Table IV). Overall, average PAM-based beaked whale density estimates across survey days were 21.5 (CV 0.50, 95% CI 20.7–22.4) or 48.6 (CV 0.44, 95% CI 47–50.9) beaked whales per 1000 km^2 , depending on whether uncertain clicks were included (Table V). The largest contribution to the overall variance was from acoustic detection probability (variance 0.06) followed by the acoustic cue counts (variance 0.02 using only “certain” detections and 0.03 for all detections).

B. Visual density estimates

Availability bias (\hat{v}) was estimated as 0.28 (CV 0.05, 95% CI 0.26–0.31) for Blainville’s beaked whales, and as 0.22 (CV 0.08, 95% CI 0.17–0.28) for Cuvier’s beaked whales (Fig. 5). Combined beaked whale \hat{v} in the survey area, averaged across proportion of groups of each species, resulted in 0.25 (CV 0.05, 95% CI 0.23–0.29). A total of 965 beaked whale group sightings were recorded during a total of 45 survey days. From those, 291 sightings were recorded by the primary platform, 310 by the secondary, and 364 (37%) by both platforms (Table VI). Among the duplicate sightings, 97 (27%) were considered “certain” and

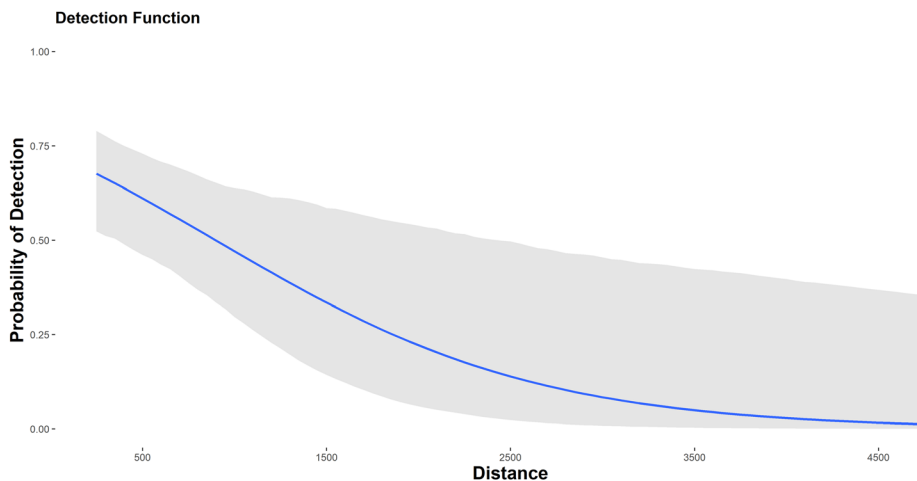


FIG. 3. (Color online) Estimated detection function for a drifting acoustic receiver placed at 200m depth in waters southwest off El Hierro. 95% confidence intervals are shown in gray. Distance is in meters.

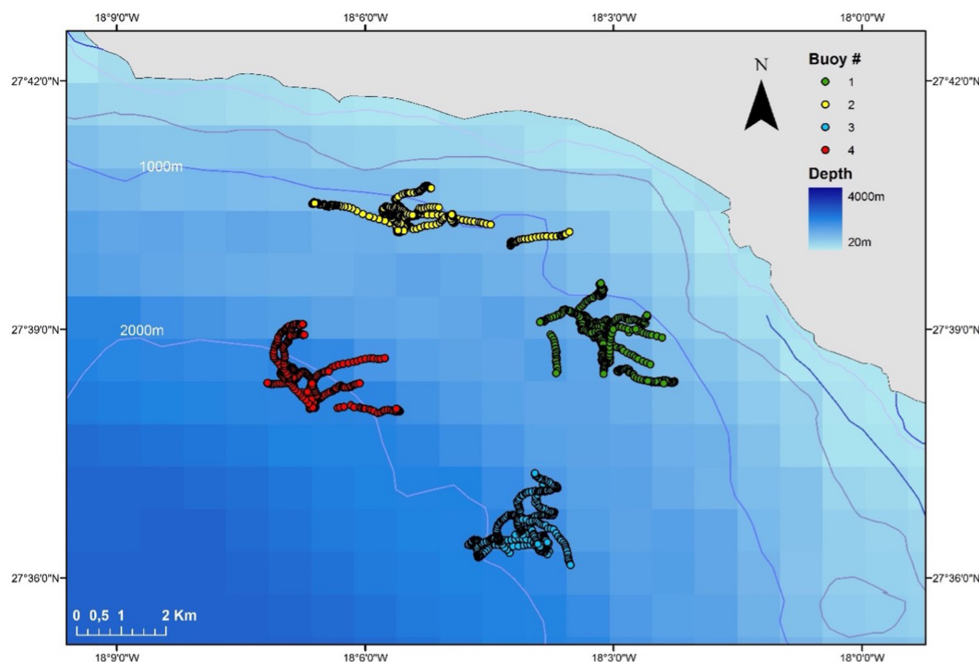


FIG. 4. (Color online) Tracks of the four SoundTrap deployed during PAM experiments in waters southwest off El Hierro. The location of each sensor, suspended at 200 m depth from a drifting buoy, was recorded with a GPS (colored dots) during daytime hours in eight survey days, between October 18 and 31, 2016. Buoys were deployed for periods ranging 4.7–7.8 h in the leeward side of the island within the 1000 and 2000 m isobaths. Buoy drift within a single survey day was <2 km.

262 (73%) “probable” duplicates. Average size of observed groups was 2.15 beaked whales (CV 0.09). Regarding the detection probability, the density gradient model with a half-normal distribution was selected as the best model to estimate the detection function (Fig. 6) (Table VII); while a beta distribution was selected to estimate the depth-dependent density function of the whales at the surface, ΔAIC of 30.13. Resulting average estimated observer’s detection probability (\hat{P}) 0.20 (CV 0.15) and associated 8 day visual density estimate of 33.7 (CV 0.77, 95% CI 8.98–50.56) beaked whales per 1000 km² (Table V). The variance for each component was largest for visual cue counts (variance 0.07), followed by visual detection probability (variance 0.01), mean group size (variance 0.008), and the whale availability (variance 0.002).

TABLE IV. Summary of beaked whale acoustic detections. Record time and total number of clicks recorded by four drifting SoundTraps deployed in the leeward off El Hierro island during a subsample of 8 days in October 2016 with click detection rate and proportion of certain beaked whale clicks. Values are means.

Date (October)	Record time (h)	Total clicks (n)	Detection rate (click h ⁻¹)	Certain detections (%)
18	6.5	5056	167.5	0.75
21	7.2	4433	131.7	0.68
22	6.7	1557	37.1	0.53
25	4.7	3704	105.6	0.62
28	6.4	4057	98.6	0.46
29	7.8	8499	199.6	0.76
30	7.2	2804	74.2	0.68
31	7.0	2760	131.0	0.77

IV. DISCUSSION

To evaluate the performance of an animal abundance estimation method, an independent true value for density or abundance is needed. Such scenarios are rare and challenging to find for most wildlife populations. Lacking true density or abundance, concurrent estimates of a species’ density–abundance obtained simultaneously using alternative methods, represent a possible approach to evaluate and validate the reliability of PAM surveys. Here, we evaluated a method currently under development for PAM-based beaked whale density estimation, using drifting autonomous recorders deployed at a predefined depth, comparing acoustic estimates to independent concurrent data based on visual density estimates obtained simultaneously from land-based point-transsects. The results of this comparison provide key evidence of the reliability of low-cost PAM surveys to study

TABLE V. Summary of detection probability and density estimates from passive acoustic monitoring and from visual surveys and reported as number of beaked whales in the survey area. Cue count “all,” all beaked whale clicks are considered; cue count “certain,” only certain beaked whale clicks were considered; \hat{P} , average detection probability and associated standard error; χ^2 , chi-square goodness-of-fit significance value. Density estimate: average density estimate (N = 9 days), 95% confidence intervals (95% CI), and associated coefficient variation (CV).

Data source	Analytical approach	\hat{P} (CV)	χ^2 p-value	Density estimate	
				mean (95% CI)	CV
Acoustic	Cue count “certain”	0.15 (0.24)	—	4.02 (3.7–3.9)	0.50
	Cue count “all”	—	—	8.65 (8.3–8.9)	0.44
Visual	Distance sampling	0.20 (0.15)	<0.001	5.8 (1.6–9.0)	0.77

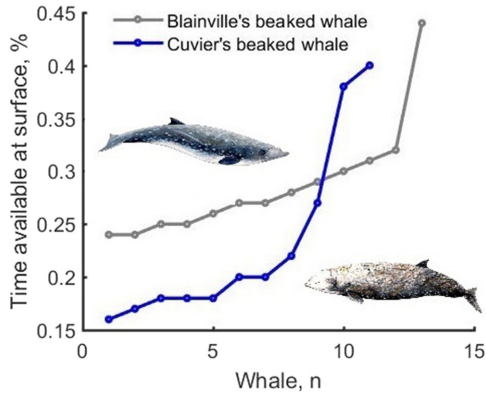


FIG. 5. (Color online) Beaked whale visual availability at the surface for tagged Blainville's (N = 12 tags, 35 dives) and Cuvier's beaked whales (N = 15 tags, 41 dives). For each tag record, whale availability as the number of 4 s periods spent at water depths <1 m over the total number of periods. Whale drawn by Chloe Yzoard (not at scale).

cryptic taxa, such as beaked whales, over relatively long time periods and in realistic scenarios.

There is a widespread increased application of PAM techniques for estimating animal density, although there are few studies in which the true number of animals in the study area is known (Phillips, 2016), to provide a means of verification of the accuracy of such estimates (reviewed by Marques *et al.*, 2013). PAM surveys have traditionally been used as either a complement or alternative to visual surveys when studying sound-producing taxa. Some cetacean species have, however, low visual detectability and, especially in these cases, acoustic methods are preferably used as they can routinely detect more animals per unit of effort than visual methods (Sebastián-González *et al.*, 2018; Thomas and Marques, 2012).

A. Acoustic density estimates

The proposed PAM method here presented provided an estimate of 21.5 or 48.6 beaked whales per 1000 km². The most conservative values (the lower estimate which considers only "certain" click detections) are not inconsistent with

TABLE VI. Summary of the visual beaked whale detections from double platform observers located in a coastal cliff in El Hierro. The number of detections is reported as the sum for both platforms. The mean beaked whale group size is reported as the average of the two shore platforms. Effort time is reported as to the number of 2min time snapshots (see Methods) per platform.

Date (October)	Effort time	Visual beaked whale detections (n)	Beaked whale group size (n)
18	224.75	23	2.17
21	223.59	76	2.42
22	215.48	7	2.09
25	164.75	8	3.39
28	209.97	10	1.77
29	254.49	44	1.75
30	223.25	35	1.88
31	218.70	44	1.75

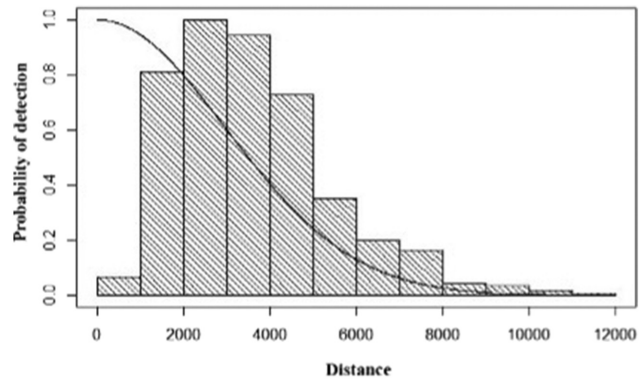


FIG. 6. Estimated detection function for land-based visual observers located on a cliff (119 m above the sea level) southwest off El Hierro. Half-normal model tested. Models were built from 935 double-observer sightings within 45 survey days. Distance is represented in meters.

concurrent visual density estimates (33.7 beaked whales per 1000 km²). Daily detections for visual and acoustic approaches showed high variance. This was expected *a priori* due to the natural variation in the number of beaked whale groups present in the area on a given day (Table VI), the environmental conditions, and the characteristics of the animals' biosonar signals; leading to a sharp decrease in detectability at distances larger than 2 km (Gkikopoulou, 2018). Increased swell height in three over eight of the selected survey days could explain the decrease in the observer's sighting rate (October 25, 28, and 29), leading to a lower abundance estimate from visual surveys in those days, compared to PAM estimates. The resulting estimates are similar to beaked whale densities obtained elsewhere using deeper static hydrophone arrays, like the ones in AUTECH (Atlantic Undersea Test and Evaluation Center, Bahamas); 22.5 or 25.3 beaked whales per 1000 km², depending on assumptions about false-positive detections (Marques *et al.*, 2009) and 24.76 beaked whales per 1000 km², when estimated >65 h after sonar exposures (see Moretti *et al.*, 2006). Such comparable results; however, do not provide information about the accuracy of the method *per se*, support similar species' density patterns across regions.

The large proportion of "uncertain" clicks detections found in the recordings led to up to 40% variation in density estimates. This is a consequence of the wide variability of

TABLE VII. Model parameter estimates describing the probability density function (pdf), $\pi_z(z; \phi)$ of beaked whale sightings with respect to seabed depth, and half-normal detection function, $g(r; \hat{\theta})$. Density models are parameterized in terms of their means ($\hat{\mu}$) and standard deviations ($\hat{\sigma}$), and $\hat{\theta}$ is the half-normal detection function parameter estimate.

Model	Probability density function parameters (pdf) ϕ	Detection function parameter $\hat{\theta}$	AIC	Δ AIC
Beta	$\hat{\mu} = 3.24; \sigma = 1.15$	2973.12	5473.36	0
Normal	$\hat{\mu} = 2061.11; \sigma = 654.48$	2992.58	5503.49	30.13
Uniform	—	4293.17	5851.59	378.23
Log-normal	$\hat{\mu} = 7; \sigma = 0.5$	2500	5953.59	480.23

detected clicks' waveforms and power spectra, which depends on the animal-sensor distance and orientation, and the random presence of other vocally active species—namely, dolphins—near the sensors (Caillat *et al.*, 2013), resulting in a lower density estimate accuracy. Gkikopoulou (2018) reported little effect of using five different detectors in the click detection rate, and therefore, here, we did not explore the effect of using different detection and classification algorithms. To improve the accuracy of density estimates without having to manually scrutinize the whole dataset (as performed in this study), particularly when it is large, it would be possible to estimate the false positive rate and proportion of “uncertain” detections from random or periodic audio samples manually analyzed throughout the recordings and use it to apply a correction to specific temporal windows.

B. Acoustic multipliers

Click production rate and click detection probability were calculated here using auxiliary DTag data from related studies and used as multipliers to convert click counts into animal density. To estimate the correct weighted mean click production rate pooled-across species present in the area, the proportion of clicks being produced by each species should be considered. In this case, mean click rates resulted very similar for each of the two species (0.46 clicks s^{-1} CV 0.03 and 0.47 clicks s^{-1} CV 0.05 for Blainvillés and Cuvier's beaked whales, respectively) and the species' proportion could have been ignored in practice. However, making explicit the calculation highlights that this is fundamental under scenarios where cue rates might differ between species. Calculations were performed assuming that there were no differences among the studied species per location and over time and using weighted averages of tag data per each recording location. Individual click rates of tagged whales has been suggested to be independent of group size for both beaked whale species (Alcázar-Treviño *et al.*, 2021). Therefore, click rates seem not to be density dependent, nor change in relation to other social parameters in this area. However, Warren *et al.* (2017) found changes over space and time in click production rate in Cuvier's beaked whales studied in Liguria and California. Potential differences in vocal behavior of this species between the Canary Islands and these areas can bias density estimates. Cue rate data from the same place and period of that of the primary survey is always preferable (Marques *et al.*, 2013); however, such concurrent *ad hoc* tag data are challenging to obtain since tags are only deployed in exceptional conditions (i.e., good weather, certain locations) and, so far, only on a limited number of species. Here, we considered measurements ($N = 41$ dive cycles) from two different locations (California and Liguria) to capture, given the data available, at least some of the natural variability in cue rates from Cuvier's beaked whales. Further studies that estimate cue rates and evaluate the variability in cue rates induced by external factors, like location, are required to evaluate the

potential bias that might remain when tags from elsewhere are used to estimate a given cue rate.

Given the characteristic vocal synchrony for these species (Aguilar de Soto *et al.*, 2020), where all individuals of the group start and end clicking within a few seconds of difference, larger groups of beaked whales do not necessarily imply variable individual click rates (driven by intra-group competition or interference) but could nonetheless result in an increase in the group's acoustic footprint, due to (i) the concurrent clicking activity of all group members, (ii) the individuals' independent movements during their deep dives' foraging phase (Aguilar de Soto *et al.*, 2020), and (iii) the distinctive high directionality of odontocete clicks (Branstetter *et al.*, 2012). However, such expanded acoustic footprint would only be registered when using various acoustic receivers covering enough radial space to effectively detect most of the clicks emitted by all group members while they forage independently, as Marques *et al.* (2019) recorded by using the AUTECH system off the Bahamas. These authors reported an increased group detected click rate as a function of group size for Blainville's, using it to estimate group size and estimating density from dive count methods. This approach has not been considered in this study, given the challenge to identify individual dives from click bouts that were found almost continuously throughout most acoustic records.

The probability of detecting a click on a hydrophone may vary depending on factors such as depth of the sensor, ambient noise, off-axis attenuation, transmission loss, and source level (SL) of the signal. Ambient noise was assumed comparable between recordings performed during the current study and the tagging experiments as the study site constitutes an area of low human impact, with little shipping activity, and both surveys were conducted in similar sea state conditions (≤ 2) and seasons (spring and autumn). Comparison of CTD (conductivity, temperature, density recorder) casts across survey periods also suggests a similar transmission of sound within ~ 150 and 850 m depth, corresponding to the average depth of the seasonal and permanent thermoclines, respectively. This depth range also comprises the depth of production of most Blainville's beaked whale clicks in this area (200–800 m) (Arranz *et al.*, 2011) and deployment of the sensors in this study (200 m). The SL and proportion of clicks emitted in an off-axis angle at different distances to the sensor are determinant of the distance at which these can be detected. The acoustic properties of clicks and the probability of detecting clicks on-axis and off-axis, because of the whale's head orientation relative to the sensor, were assumed to be comparable across surveys, given that samples come from the same beaked whale population and sensors were located at similar seabed depth and distance from the coast (Reyes, 2018; Gkikopoulou, 2018). The detection function was estimated as a function of horizontal distance, where clicks detected on the receivers are recorded as presences and the clicks not detected as absences, with an empirical detection function calculated by dividing the number of clicks detected by the total number

of clicks produced (Gkikopoulou, 2018). As is recommendable in distance sampling applications, the horizontal distance was used instead of the slant distance, integrating all the possible slant distances for animals vocalizing at different depths.

Non-acoustical factors affecting the click detection probability involve the probability that a whale is in the area within the effective detection distance of the PAM system. If beaked whale spatial density (non-uniform distribution) was not considered, acoustic density estimates averaged 70 whales (range 55.3–84.8), a value an order of magnitude larger than results obtained from visual observations in the same area, and more than double of those reported in other areas with comparable resident beaked whale populations (see Moretti *et al.*, 2006; Marques *et al.*, 2009). This underlines the importance of considering non-uniform animal distributions when estimating the acoustic detection probability on PAM surveys and collecting prior information on animal distribution, particularly in areas with steep bathymetry or sudden changes in habitat conditions where a density gradient is likely to occur. Cuvier's beaked whales have been reported to perform extreme dives amongst all breath-hold divers (Schorr *et al.*, 2014), and noticeably the likelihood of detecting beaked whale clicks is likely to decrease with the difference between the depth of the whale and sensor depth (Barlow *et al.*, 2013; Gkikopoulou, 2018). On the other hand, track line acoustic detection probability for Cuvier's beaked whales seems to be higher compared to Blainville's beaked whales (Barlow *et al.*, 2013), probably due to its shorter dive cycles (Warren *et al.*, 2017). Given that the point transect acoustic detection function applied here is based on trials with tagged Blainville's beaked whales, our density estimates of detectability (applied to the combined data for both beaked whale species) might be biased low, and hence, density estimates could potentially be biased upwards.

C. Visual validation approach

While conducting the acoustic surveys, the study area was simultaneously monitored by two land-based visual platforms to obtain a concurrent independent estimate of abundance–density. Conventional visual distance sampling techniques assume (i) uniform animal density with respect to the samplers based on a random sampling design, (ii) animals being detected at their initial locations, and (iii) certain detection on the track line or point-transect, that is $g(0) = 1$ (Buckland *et al.*, 2001; Chen, 2000; Laake *et al.*, 2011). Such techniques are not appropriate to estimate detection probability of beaked whales from fixed points on land (Buckland *et al.*, 2006) for two reasons: (i) beaked whales spend most of the time underwater and not available for detection even when they are at close distance, and (ii) they exhibit a depth preference leading to a non-uniform distribution relative to the coast (Arranz *et al.*, 2011; Tyack *et al.*, 2006).

The Chi-square goodness-of-fit test (p -value < 0.001) suggested that sightings do not fit the predicted density model proposed by Arranz *et al.* (2013). One possible explanation for this is that the species have a seasonally dependent distribution, as the dataset used by Arranz *et al.* (2013) spanned three seasons over 5 yr ($N = 1789$ sightings) and in this study, data were collected in October 2016 ($N = 191$ sightings). This model provided an abundance estimate of 5.9 (95% CI 1.6–9.0) beaked whales in the study area, the greatest similarity with PAM density estimates, considering “certain” detections. Despite this similarity, we acknowledge some bias in density estimates derived from this model may be present, due to failure of the assumption of perfect detectability at distance 0 from the observer. Nonetheless, the density gradient model allowed data to be collected with relatively low effort, since a single observer platform is needed and provided more accurate density estimates compared to MR methods. Further ongoing efforts combining MR and density gradient approaches will certainly improve estimates of beaked whale density from land-based point-transect visual surveys.

V. CONCLUSIONS

The PAM method presented here provides estimates of whale density using low-cost mobile recording platforms and match concurrent density estimates obtained using independent visual data. While two independent simultaneous methods do not necessarily definitely constitute mutual validation, the most parsimonious explanation for providing comparable results is that overall, they are reliable, assuming there are no major assumption violations in the estimates from the two different methods. Further work that focuses on generating depth-dependent spatial density distribution data using PAM to correct detection probability would improve density estimates of point-transect PAM surveys when animal distribution is not uniform. Obtaining *in situ* detection functions and sound production rates is fundamental for real-time monitoring studies and would contribute to the progress of PAM methodology. These results have implications, not only on the long-term monitoring of potential anthropogenic disturbance on beaked whales, but also on the evaluation of the number of animals at risk to prevent or minimize possible accidental exposures during naval operations.

ACKNOWLEDGMENTS

We acknowledge field assistants for their help in data collection, particularly to Eva Hidalgo, Alberto Sarabia, Jacobo Marrero, Chloe Yzoard, Agus Schiavi, and Alejandro Escáñez. We thank Mark Johnson, Doug Gillespie, Marjolaine Caillat, John Atkins, and Francisco Barreto for technical advice, Victoria Warren for contributing with Cuvier's metadata, and Cabildo of El Hierro for providing access to facilities. P.A., D.M., K.G., T.A.M., A.C., and field work were funded by Office of Naval Research award #N000141612973 and research

conducted under Spanish Ministry permit #28606/2016 and Canary government permit # 421373/2016. T.A.M. is thankful for partial support by CEAUL (funded by Fundação para a Ciência e a Tecnologia, Portugal, through the project UIDB/00006/2020) and time under the ACCURATE project funded by the U.S. Navy Living Marine Resources program (Contract #N3943019C2176). We are grateful to associate editor Aaron Thode and an anonymous reviewer for their comments and suggestions, which led to a much stronger paper. The datasets generated during the current study are available in the Dryad repository.

¹See supplementary material at <https://www.scitation.org/doi/suppl/10.1121/10.0017921> for raw data used to estimate Blainville's and Cuvier's beaked whale click production, dive cycle length, and the resulting click rate from DTag recordings. For a description of the general method and equations used to estimate a probability density function and visual detection probability for beaked whale groups from land-based observations.

- Aguilar de Soto, N. A., Visser, F., Tyack, P. L., Alcazar, J., Ruxton, G., Arranz, P., Madsen, P., and Johnson, M. (2020). "Fear of killer whales drives extreme synchrony in deep diving beaked whales," *Sci. Rep.* **10**, 1–9.
- Akaike, H. (1973). "Information theory and an extension of the maximum likelihood principle," in *2nd International Symposium on Information Theory*, edited by B. N. Petrov and F. Csaki (Akademia Kiado, Budapest), pp. 267–281.
- Alcázar-Treviño, J., Johnson, M., Arranz, P., Warren, V. E., Pérez-González, C. J., Marques, T., Madsen, P. T., and Aguilar de Soto, N. (2021). "Deep-diving beaked whales dive together but forage apart," *Proc. R. Soc. B.* **288**, 20201905.
- Aodha, O., Gibb, R., Barlow, K. E., Browning, E., Firman, M., Freeman, R., and Pandourski, I. (2018). "Bat detective—Deep learning tools for bat acoustic signal detection," *PLoS Comput. Biol.* **14**, e1005995.
- Arranz, P., Aguilar Soto, N., Madsen, P. T., Brito, A., Bordes, F., and Johnson, M. (2011). "Following a foraging fish-finder: Diel habitat use of Blainville's beaked whales revealed by echolocation," *PLoS One* **6**, e28353.
- Arranz, P., Borchers, D. L., Aguilar de Soto, N., Johnson, M. P., and Cox, M. J. (2013). "A new method to study inshore whale cue distribution from land-based observations," *Mar. Mam. Sci.* **30**, 810–818.
- Barlow, J., Moore, J. E., McCullough, J. L. K., and Griffiths, E. T. (2022). "Acoustic-based estimates of Cuvier's beaked whale (*Ziphius cavirostris*) density and abundance along the U.S. West Coast from drifting hydrophone recorders," *Mar. Mammal Sci.* **38**(2), 517–538.
- Barlow, J., Tyack, P. L., Johnson, M. P., Baird, R. W., Schorr, G. S., Andrews, R. D., and Aguilar de Soto, N. (2013). "Trackline and point detection probabilities for acoustic surveys of Cuvier's and Blainville's beaked whales," *J. Acoust. Soc. Am.* **134**, 2486–2496.
- Borchers, D. L., and Efford, M. G. (2008). "Spatially explicit maximum likelihood methods for capture-recapture studies," *Biometrics* **64**, 377–385.
- Borchers, D. L., Zucchini, W., and Fewster, R. M. (1998). "Mark-recapture models for line transect surveys," *Biometrics* **54**, 1207–1220.
- Branstetter, B. K., Moore, P. W., Finneran, J. J., Tormey, M. N., and Aihara, H. (2012). "Directional properties of bottlenose dolphin (*Tursiops truncatus*) clicks, burst-pulse, and whistle sounds," *J. Acoust. Soc. Am.* **131**, 1613–1621.
- Buckland, S., Anderson, D., Burnham, K., Laake, J., Borchers, D., and Thomas, L. (2001). *Introduction to Distance Sampling: Estimating Abundance of Biological Population*. (Oxford University Press, Oxford, UK).
- Buckland, S. T. (2006). "Point-transect surveys for songbirds: Robust methodologies," *Auk* **123**, 345–357.
- Buckland, S. T., Rexstad, E. A., Marques, T. A., and Oedekoven, C. S. (2015). *Distance Sampling: Methods and Applications* (Springer, New York).
- Caillat, M. (2018). (private communication).
- Caillat, M., Thomas, L., and Gillespie, D. (2013). "The effects of acoustic misclassification on cetacean species abundance estimation," *J. Acoust. Soc. Am.* **134**, 2469–2476.
- Cato, D. H. (1998). "Simple methods of estimating source levels and locations of marine animal sounds," *J. Acoust. Soc. Am.* **104**, 1667–1678.
- Chen, S. X. (2000). "Animal abundance estimation in independent observer line transect surveys," *Environ. Ecological Stat.* **7**, 285–299.
- Cox, T. M., Ragen, T. J., Read, A. J., Vos, E., Baird, R. W., Balcomb, K., and Benner, L. (2006). "Understanding the impacts of anthropogenic sound on beaked whales," *J. Cetacean Res. Manage.* **7**, 177–187.
- Cox, M. J., Borchers, D. L., and Kelly, N. (2013). "nupoint: An R package for density estimation from point transects in the presence of nonuniform animal density," *Methods Ecol. Evol.* **4**, 589–594.
- Deichmann, J. L., Hernández-Serna, A., Delgado, J. A., Campos-Cerqueira, C. M., and Aide, T. M. (2017). "Soundscape analysis and acoustic monitoring document impacts of natural gas exploration on biodiversity in a tropical forest," *Ecol. Indic.* **74**, 39–48.
- Gillespie, D., Mellinger, D. K., Gordon, J., McLaren, D., Redmond, P., McHugh, R., Trinder, P. W., Deng, X.-Y., and Thode, A. (2009). "PAMGUARD: Semiautomated, open-source software for real-time acoustic detection and localisation of cetaceans," *J. Acoust. Soc. Am.* **125**, 2547.
- Gkikopoulou, K. (2018). "Getting below the surface: Density estimation methods for deep diving animals using slow autonomous underwater vehicles," Ph.D. thesis, University of St Andrews, St Andrews, UK.
- Hagens, S. V., Rendall, A. R., and Whisson, D. A. (2018). "Passive acoustic surveys for predicting species' distributions: Optimising detection probability," *PLoS One* **13**, e0199396.
- Hildebrand, J. A., Baumann-Pickering, S., Frasier, K. E., Trickey, J. S., Merckens, K. P., Wiggins, S. M., McDonald, M. A., Garrison, L. P., Harris, D., Marques, T. A., and Thomas, L. (2015). "Passive acoustic monitoring of beaked whale densities in the Gulf of Mexico," *Sci. Rep.* **5**, 16343.
- Horvitz, D. G., and Thompson, D. J. (1952). "A generalization of sampling without replacement from a finite universe," *J. Am. Statist. Assoc.* **47**(260), 663–685.
- Johnson, M., Madsen, P. T., Zimmer, W. M. X., Aguilar Soto, N., and Tyack, P. L. (2006). "Foraging Blainville's beaked whales (*Mesoplodon densirostris*) produce distinct click types matched to different phases of echolocation," *J. Exp. Biol.* **209**, 5038–5050.
- Johnson, M. P., and Tyack, P. L. (2003). "A digital acoustic recording tag for measuring the response of wild marine mammals to sound," *IEEE J. Ocean. Eng.* **28**, 3–12.
- Küsel, E. T., Siderius, M., and Mellinger, D. K. (2016). "Single-sensor, cue-counting population density estimation: Average probability of detection of broadband clicks," *J. Acoust. Soc. Am.* **140**, 1894–1903.
- Laake, J. L., Collier, B. A., Morrison, M. L., and Wilkins, R. N. (2011). "Point-based mark-recapture distance sampling," *J. Agric., Biol., Environ. Stat.* **16**, 389–408.
- Lerczak, J. A., and Hobbs, R. C. (1998). "Calculating sighting distances from angular readings during shipboard, aerial, and shore-based marine mammal surveys," *Mar. Mammal Sci.* **14**, 590–599.
- Marques, T. A., Buckland, S., Borchers, D. L., Tosh, D., and McDonald, R. (2010). "Point transect sampling along linear features," *Biometrics* **66**, 1247–1255.
- Marques, T. A., Jorge, P. A., Mouriño, H., Thomas, L., Moretti, D. J., Dolan, K., and Dunn, C. (2019). "Estimating group size from acoustic footprint to improve Blainville's beaked whale abundance estimation," *Appl. Acoust.* **156**, 434–439.
- Marques, T. A., Thomas, L., Martin, S. W., Mellinger, D. K., Ward, J. A., Moretti, D. J., Harris, D., and Tyack, P. L. (2013). "Estimating animal population density using passive acoustics," *Biol. Rev.* **88**, 287–309.
- Marques, T. A., Thomas, L., Ward, J., DiMarzio, N., and Tyack, P. L. (2009). "Estimating cetacean population density using fixed passive acoustic sensors: An example with Blainville's beaked whales," *J. Acoust. Soc. Am.* **125**, 1982–1994.
- Moretti, D., DiMarzio, N., Morrissey, R., Ward, J., and Jarvis, S. (2006). "Estimating the density of Blainville's beaked whale (*Mesoplodon*

- densirostris*) in the Tongue of the Ocean (TOTO) using passive acoustics," in *Oceans 2006*, pp. 1–5.
- Phillips, G. (2016). "Passive acoustics: A multifaceted tool for marine mammal conservation," Ph.D. thesis, Duke University, Durham, NC.
- R Core Team (2022). "R: A language and environment for statistical computing." R Foundation for Statistical Computing, Vienna, Austria, <https://www.R-project.org/> (Last viewed April 1, 2022).
- Reyes, C. (2018). "Abundance estimate, survival and site fidelity patterns of Blainville's (*Mesoplodon densirostris*) and Cuvier's (*Ziphius cavirostris*) beaked whales off El Hierro (Canary Islands)," MPhil. thesis, St Andrews University, St Andrews, UK.
- Schorr, G. S., Falcone, E. A., Moretti, D. J., and Andrews, R. D. (2014). "First long-term behavioral records from Cuvier's beaked whales (*Ziphius cavirostris*) reveal record-breaking dives," *PLoS One* **9**, e92633.
- Schweder, T., and Hjort, N. (1996). *Bayesian Synthesis or Likelihood Synthesis-What Does the Borel Paradox Say?* (Oslo University, Department of Economics, Memorandum).
- Sebastián-González, E., van Aardt, J., Sacca, K., Barbosa, J. M., Kelbe, D., and Hart, P. J. (2018). "Testing the acoustic adaptation hypothesis with native and introduced birds in Hawaiian forests," *J. Ornithol.* **159**, 827–838.
- Seber, G. A. F. (1982). *The Estimation of Animal Abundance, and Related Parameters*, 2nd ed. (Macmillan Publishing Co., New York).
- Thomas, L., and Marques, T. A. (2012). "Passive acoustic monitoring for estimating animal density," *Acou. Today* **8**, 35–44.
- Tyack, P. L., Johnson, M., Soto, N. A., Sturlese, A., and Madsen, P. T. (2006). "Extreme diving of beaked whales," *J. Exp. Biol.* **209**(21), 4238–4253.
- Tyack, P. L., Johnson, M. P., Zimmer, W. M. X., De Soto, N. A., and Madsen, P. T. (2006). "Acoustic behavior of beaked whales, with implications for acoustic monitoring," in *Oceans, 2006*, pp. 1–6.
- Ward, J., Jarvis, S., Moretti, D., Morrissey, R., DiMarzio, N., Johnson, M., and Marques, T. (2011). "Beaked whale (*Mesoplodon densirostris*) passive acoustic detection in increasing ambient noise," *J. Acoust. Soc. Am.* **129**, 662–669.
- Warren, V. E., Marques, T. A., Harris, D., Thomas, L., Tyack, P. L., Aguilar Soto, N., and Johnson, M. P. (2017). "Spatio-temporal variation in click production rates of beaked whales: Implications for passive acoustic density estimation," *J. Acoust. Soc. Am.* **141**, 1962–1974.
- Williams, B. K., Nichols, J. D., and Conroy, M. J. (2002). *Analysis and Management of Animal Populations: Modeling, Estimation, and Decision Making* (Academic Press, San Diego).
- Zimmer, W. M. X., Johnson, M., Madsen, P. T., and Tyack, P. (2005). "Echolocation clicks of free-ranging Cuviers beaked whales (*Ziphius cavirostris*)," *J. Acoust. Soc. Am.* **117**, 3919–3927.